Electronic Measurements of Single-Molecule Processing by DNA Polymerase I (Klenow Fragment)

Tivoli J. Olsen,[†,‡] Yongki Choi,[§,‡] Patrick C. Sims,[§] O. Tolga Gul,[§] Brad L. Corso,[§] Chengjun Dong,[§] William A. Brown,[†] Philip G. Collins,*[,§] and Gregory A. Weiss*[,†,⊥]

Departments of [†]Chemistry, [§]Physics and Astronomy, and [⊥]Molecular Biology, University of California, Irvine, California 92697, United States

Ⓢ *Supporting Information*

ABSTRACT: Bioconjugating single molecules of the Klenow fragment of DNA polymerase I into electronic nanocircuits allowed electrical recordings of enzymatic function and dynamic variability with the resolution of individual nucleotide incorporation events. Continuous recordings of DNA polymerase processing multiple homopolymeric DNA templates extended over 600 s and through >10 000 bond-forming events. An enzymatic processivity of 42 nucleotides for a template of the same length was directly observed. Statistical analysis determined key kinetic parameters for the enzyme's open and closed conformations. Consistent with these nanocircuit-based observations, the enzyme's closed complex forms a phosphodiester bond in a highly efficient process >99.8% of the time, with a mean duration of only 0.3 ms for all four dNTPs. The rate-limiting step for catalysis occurs during the enzyme's open state, but with a nearly 2-fold longer duration for dATP or dTTP incorporation than for dCTP or dGTP into complementary, homopolymeric DNA templates. Taken together, the results provide a wealth of new information complementing prior work on the mechanism and dynamics of DNA polymerase I.
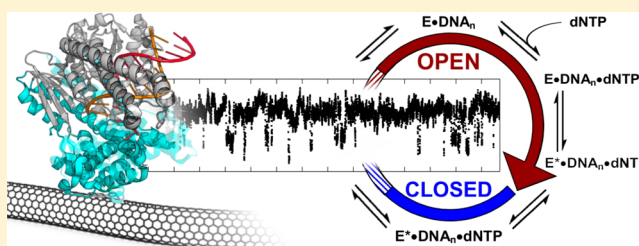
■ INTRODUCTION

All forms of life require DNA polymerases for the accurate replication and repair of DNA. Although sequences of DNA polymerases vary, all DNA polymerases operate through a common, conserved mechanism.[1,2] Such enzymes typically have exceptionally low error rates (e.g., Klenow fragment, or KF, of DNA polymerase I incorporates one error in ~10^5 bases[3−5]). To achieve this fidelity, DNA polymerases have evolved a stepwise mechanism in which a series of elementary reactions and structural rearrangements serve as kinetic checkpoints.[6] However, intense investigation of this mechanism using ensemble and single-molecule techniques has not yet resolved fundamental aspects,[2] such as the details of critical subcomponent steps including nucleotide recognition, error checking, or translocation.

DNA polymerase incorporates deoxynucleotides (dNTPs) into a complementary template strand under the direction of a single-stranded DNA template. The nascent strand is lengthened base-by-base as the enzyme catalyzes nucleophilic attack of the new strand's 3′-hydroxyl terminus with the α-phosphate of the incoming dNTP.[7] Figure 1a shows a minimum scheme[6] for important kinetic steps occurring during one cycle of this process. In the first step, the enzyme's "thumb" domain binds a primer-template DNA to form a binary open complex, E·DNA$_n$. Successful recognition of a complementary nucleotide triphosphate allows the enzyme's "fingers" subdomain to snap closed on the activated ternary complex, E*·DNA$_n$·dNTP. This rapid conformational transition has been directly observed by numerous single-molecule Förster resonance energy transfer (smFRET) experiments[8−15] and inferred from co-crystal X-ray structures.[16,17] After nucleotide incorporation, DNA polymerase can either translocate along the DNA template to begin a new cycle or dissociate from the template.[18,19]

Unknown or contested aspects of this cycle include the kinetic rates of each elementary step, the chemical nature of the rate-limiting step, and the precise step in which the fingers subdomain reopens. Furthermore, reported values for KF processivity have a wide range from 1 to 50 bases; the lower values result from a template dissociation probability as high as 13% per cycle.[18,20−23] Also, some researchers report KF replication rates that differ for purine and pyrimidine bases,[9,23,24] indicating that one or more rate constants may be nucleotide-dependent.

Single-molecule techniques are promising ways to resolve such issues, since they have proven to be effective at revealing enzyme dynamics and resolving transient intermediate states hidden to ensemble measurements.[25,26] The most common single-molecule method, smFRET, has been widely applied to KF, a model system for DNA polymerase.[8−15] However, smFRET has limited resolution of very fast events[27] and no capacity for long-duration monitoring of a single molecule.[28] For example, no smFRET measurement has measured more
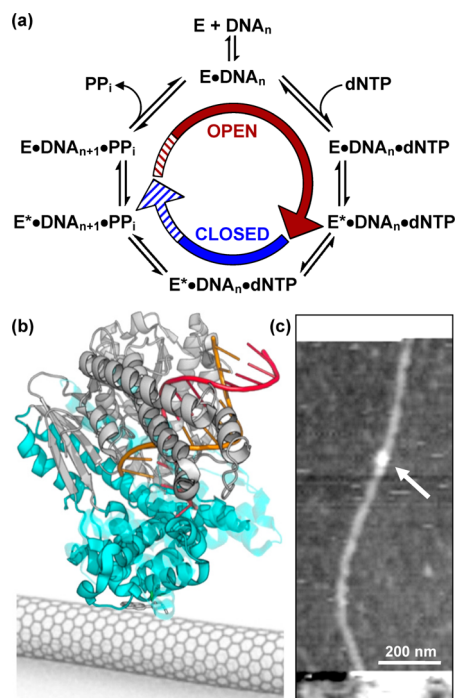
Figure 1. Electrically monitoring the catalytic cycle of Klenow fragment. (a) The minimum reaction pathway of KF, showing each key step in DNA polymerization and the primary accompanying mechanical motion. Hatched sections indicate uncertainties in the alignment between chemical and mechanical steps. (b) Schematic of a single-walled carbon nanotube with an attached KF molecule, the motions of which transduce electrical signals. Non-covalent attachment is accomplished through a single cysteine engineered into the fingers domain (cyan). The image depicts closed and open (translucent) structures of a homologous DNA polymerase (*B. stearothermophilius*, PDB: 1L3U and 1LV5), a template strand (red), and the growing primer strand (orange). (c) Example atomic force micrograph of a 2-nm-diameter SWNT device with a single KF attachment (∼7 nm, arrow). Horizontal bands at the top and bottom indicate the protective polymer layer, under which the SWNT connects to metallic electrodes.

than three successive nucleotide incorporation events by the same KF molecule.[9] Rather than focusing on enzyme turnover, several smFRET experiments used a dideoxy substrate, which elegantly probes conformational dynamics during molecular recognition of the nucleotide.[12,15]

Here, we have applied a new and label-free single-molecule technique to continuously monitor KF activity by the same molecule for long durations and multiple turnovers. Our approach bypasses the limitations of smFRET by monitoring the enzyme electronically, using a single-walled carbon nanotube (SWNT) field effect transistor (FET) device. This technique was previously demonstrated using individual lysozyme molecules bioconjugated to SWNT FETs.[29,30] In that case, lysozyme activity induced dynamic changes in the FET current $I(t)$, and analysis of the $I(t)$ fluctuations reproduced rates measured by smFRET and ensemble experiments[31−34] while also providing new measurements of lysozyme's processivity and dynamic disorder.

In this report, the electronic monitoring technique has been used to study processive DNA synthesis by KF. With a single KF molecule attached to a SWNT FET transducer, measurements could extend for many minutes and resolve individual nucleotide incorporation for >10 000 events. This monitoring

of KF clearly distinguishes two different conformations dependent on the base pair formed, and demonstrates that the rate-determining step occurs during the enzyme's open conformation. Furthermore, the rates were 45% slower for dTTP or dATP than for dCTP or dGTP nucleotide incorporation into complementary, homopolymeric DNA templates.

EXPERIMENTAL SECTION

The measurements reported here investigated the activity of a variant of the exonuclease-deficient[35] Klenow fragment of DNA polymerase I (D355A/E357A/L790C/C907S), hereafter referred to as KF. The KF variant was engineered by oligonucleotide site-directed mutagenesis followed by overexpression and purification from *E. coli* to >90% homogeneity (Supporting Information (SI), Figure S1). This variant of KF was designed to have a single cysteine at residue 790 near the highly mobile fingers subdomain for bioconjugation to the SWNT, following reaction with pyrene-maleimide as described previously.[29,30] This position places the SWNT close to a region undergoing dramatic conformational changes during the opening and closing of the enzyme.[17] (Figure 1b). Specific incubation and rinsing protocols were used to obtain devices having one attached pyrene-modified KF molecule with an 84% success rate (protocols provided in the SI). Completed devices were typically imaged by in-liquid atomic force microscopy (AFM) prior to electronic measurements to ensure single-enzyme attachments (Figure 1c).

A fluorescence-based, ensemble assay tested the pyrene-maleimide-modified KF activity under steady-state conditions (Figures S2 and S3). Following reaction with pyrene-maleimide, KF had activity about 33% lower than that of the unmodified, wild-type KF. The wild-type KF in this experiment also had mutations (D355A/E357A) to abrogate its exonuclease activity. Thus, the KF applied in the electronic measurements reported here could remain active following bioconjugation to pyrene-maleimide.

After fabrication, KF-labeled SWNT FETs were measured in a standard buffered solution (10 mM Tris, 50 mM NaCl, 10 mM MgCl$_2$, 10 mM DTT, pH 7.8). $I(t)$ was continuously recorded for no less than 600 s with the drain−source and liquid gate−source potentials held constant at 100 and 0 mV, respectively. A single KF device was measured with and without the following homopolymeric templates fused to a standard M13 priming site: poly(dA)$_{42}$, poly(dT)$_{42}$, poly(dG)$_{42}$, or poly(dC)$_{42}$ (100 nM, unless otherwise indicated). After hybridization with the M13 forward primer (100 nM), either complementary or non-complementary dNTPs (10 μM) were added. To avoid cross-contamination of templates, the KF-tethered nanocircuit was rinsed extensively with buffer before the addition of each new template solution.

RESULTS AND DISCUSSION

When both a homopolymeric DNA template and its complementary dNTP were present in the surrounding buffer solution, 21 different KF-SWNT devices all reliably exhibited stochastic pulse trains with brief excursions of $\Delta I(t)$ below the mean baseline currents. Figure 2a,b shows the typical $\Delta I(t)$ excursion during extended recordings from one KF-conjugated device in poly(dA)$_{42}$ and poly(dC)$_{42}$ templates, respectively, and complementary dNTPs. In every measurement, the $\Delta I(t)$ excursions disappeared when the complementary dNTPs were absent, replaced by non-complementary dNTPs or complementary dideoxyribonucleotides (ddNTPs). In addition, excursions were unobserved for KF-conjugated devices treated with dNTPs in the absence of a DNA template. These and additional negative control measurements are shown in Figures S5−S7. Because the enzyme can adopt a closed conformation only in the presence of both DNA template and complementary dNTP,[17] the $\Delta I(t)$ excursions correlate with KF
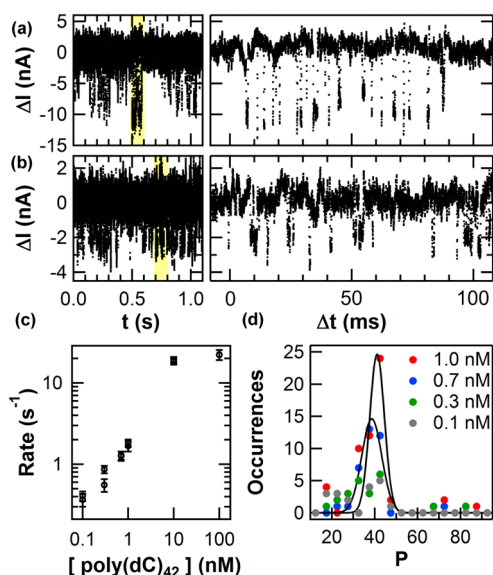
Figure 2. Electronic detection of nucleotide incorporation events. (a) One second of $\Delta I(t)$ recordings in the presence of poly(dA)$_{42}$ template and complementary dTTP. The region highlighted in yellow is magnified on the right. (b) A similar recording from the same device processing a poly(dC)$_{42}$ template in the presence of dGTP. (c) The average number of ΔI excursions per second at six different concentrations of poly(dC)$_{42}$ with dGTP (10 μM). The results from two independent devices (shown in closed square and open circle) are indistinguishable at most concentrations. (d) A histogram of P, the number of ΔI excursions occurring between pauses due to template dissociation. The peak in P is equal to the length of the unpaired bases in the DNA template·primer used in this experiment. As described in the text, short clusters could not be distinguished from noise in the SWNT FET circuit, and are thus omitted from the histogram and the analysis.

opening and closing during processive nucleotide incorporation events.

The rates of $\Delta I(t)$ excursions exhibit dose dependent response to the template concentration (Figure 2c). At both 10 and 100 nM of poly(dC)$_{42}$ template, the excursions maintained a relatively constant rate of 20 s^{-1}. This rate represents a complete catalytic cycle in Figure 1, and compares favorably with ensemble-measured catalytic rates.[36,37] At template concentrations below the dissociation constant of the KF·template complex (K_d = 5 nM),[36,37] the enzyme must wait for a new template to bind, and the time-average rate varies linearly with the template concentration (Figure 2c). At template concentrations around 0.1 nM, long periods of inactivity, 30 s or longer, were interrupted by clusters of excursions (Figure S8).

Within such clusters of $\Delta I(t)$, the mean frequency of $\Delta I(t)$ excursions remained approximately 20 s^{-1}, recapitulating the excursion rate observed under V_{max} conditions. Thus, the time-averaged rates in Figure 2c include two components. First, clusters of $\Delta I(t)$ excursions have rates characteristic of enzyme activity. Such clusters occur upon template binding to KF, and end when the template dissociates. Second, as a result of diffusion-dependent waiting times for the template to reach the enzyme, quiet periods decrease the time-averaged rates.

To demonstrate that each $\Delta I(t)$ excursion corresponds to a single dNTP incorporation, we measured the number of $\Delta I(t)$ excursions per template strand under template-limited conditions (Figure 2d). At template concentrations of 1 nM

or less, these clusters were clearly separated by quiet, inactive periods; under this condition, the number of excursions, P, during a single cluster could be easily counted. The best balance between reasonable statistics (tens of events) and significant waiting times (3 s on average) occurred at a template concentration of 1 nM. At this concentration, P peaked at 42 $\Delta I(t)$ excursions per template molecule, with almost no clusters having more events. The histogram peak matched the 42 unpaired bases of the DNA template. The number of $\Delta I(t)$ excursions observed from the processing of a single template molecule was equal to the number of unpaired bases in the DNA template, and no $\Delta I(t)$ excursions are observed in the presence of a complementary ddNTP. Therefore, each individual $\Delta I(t)$ excursion below the baseline current corresponds to exactly one dNTP incorporation.

Similar conclusions were reached using shorter, poly(dA)$_{10}$ templates. However, data sets from short templates proved more difficult to analyze. When separated by 10−30 s, clusters of a few $\Delta I(t)$ excursions were indistinguishable from SWNT noise generated by other mechanisms, such as nonspecific binding events (Figure S4). Because of the difficulty in distinguishing short clusters from noise, Figure 2d does not extend below a cluster size of 10. Thus, we cannot rule out the possibility of a second peak below 10 bases, and the experiments reported here do not assess the maximal or average processivity of KF. In the context of an enzyme with a range of reported processivity values,[20−23] we observe the processive incorporation of at least 42 dNTPs, which reflects the 42 unpaired bases of the DNA templates used in our experiments.

Previous SWNT FET measurements using lysozyme identified substrate-induced mechanical motions by the enzyme as the primary cause of $\Delta I(t)$ excursions.[29,30] Nucleotide incorporation occurs after closing of the fingers subdomain;[12] in X-ray crystal structures, both template and complementary dNTP binding are required for KF to access its closed conformation.[17] Therefore, we assign the low- and high-current states of the FET to correspond to the fingers-closed and fingers-opened conformations of KF, respectively. This low current excursion upon enzyme closure could result from either positively charged side-chain functionalities moving closer to or negatively charged functionalities moving away from the SWNT.

KF-catalyzed dNTP incorporation is a highly efficient process as indicated by the nearly one-to-one correspondence of the template length with the number of $\Delta I(t)$ excursions. Enzyme closures resulting in failed dNTP incorporations would extend the histogram in Figure 2d past 42 base pairs. More than 42 closures were observed in <4% of the clusters, suggesting that, when KF closes, a dNTP in incorporated with a 99.8% success rate.

The slower step of dNTP recognition, which includes the release of mismatched dNTPs, must occur before closure of the fingers subdomain. Therefore, the rate-limiting, non-covalent binding step[37,38] occurs during the enzyme's open conformation. Notably, we did not observe any closed KF in the absence of the correct dNTP or in the presence of a complementary chain terminating ddNTP (Figures S5−S7). However, under such conditions, any small $\Delta I(t)$ excursions were indistinguishable from noise. Thus, unlike smFRET studies that find a significant rate of enzyme closure under similar circumstances,[12,15] the approach reported here can only assess a catalytically committed conformation.

Next, we describe the statistical analysis of the low- and high-current states from many thousands of KF closures recorded under V_{max} conditions with the 42-mer homopolymeric DNA templates described above (Figure 3). Each closure, repre-
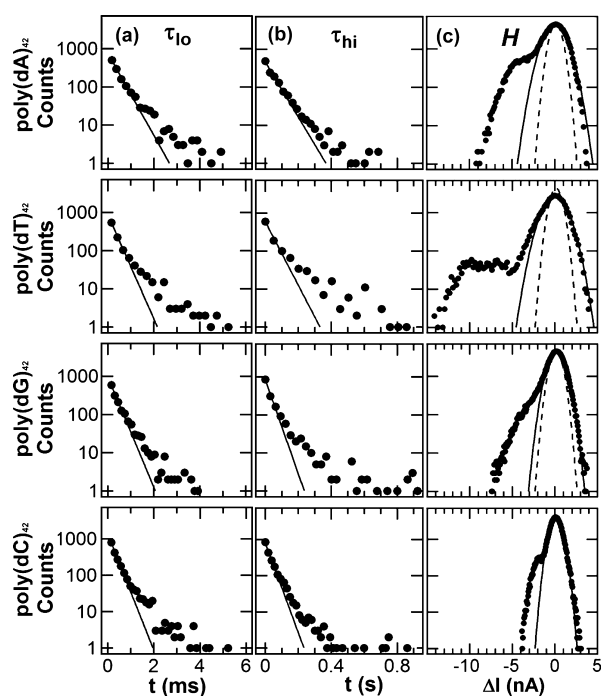

Figure 3. Parameter distributions accumulated from 100 s of processing. (a) Histogram of τ_{lo} durations for each of four homopolymeric DNA templates in the presence of a complementary dNTP. Exponential fits are shown as solid lines. (b) Histogram of τ_{hi} durations. (c) Histogram of $\Delta I(t)$ recordings, with solid lines indicating Gaussian fits to fluctuations of the open conformation centered around $\Delta I = 0$. Enzyme closures cause the shoulder of events to the left of each main peak. Dashed lines in each panel indicate the minimum peak width observed using poly$(dC)_{42}$ to emphasize the effect of different substrates on the open enzyme.

sented by a single $\Delta I(t)$ excursion, can be described by the following three independent parameters: the duration τ_{lo} of the time spent in the enzyme's closed conformation, the duration τ_{hi} of the time spent in the enzyme's open conformation, and the average height H of each $\Delta I(t)$ excursion. From expansion of the x-axes (right, Figure 2a,b), the magnitudes and durations of these parameters are apparent during typical KF closures.

Figure 3 shows distributions for all three parameters, as determined for each of the four homopolymeric DNA templates with their complementary dNTPs. All eight τ distributions are derived from 100-s segments of data. The distributions reasonably fit simple Poisson distributions having single $\langle \tau \rangle$ time constants, and a single exponential fit encompasses >95% of events observed to provide reliable

statistics to approximate enzyme activity. Averages and standard deviations of each distribution are summarized in Table 1.

The mean duration of the closed complex $\langle \tau_{lo} \rangle$ was measured to be 0.3−0.4 ms for the four homopolymeric DNA templates (Figure 3a). Generalizing this result, we conclude that phosphoryl transfer, which occurs during the closed state of the enzyme,[17,19] is an extremely rapid and efficient process, and its mechanism is largely independent of the specific dNTP. At 0.42 ms, the incorporation of dTTP into the poly$(dA)_{42}$ template is statistically longer than the other template-dNTP base pairs.

To further examine the dynamics during this stage of the catalytic cycle, the variance of τ_{lo} can be used to assess the number of rate-limiting steps taking place as the enzyme opens. A mean-normalized variance $r = \sigma^2/\langle \tau \rangle^2 = 1$ indicates a duration that is rate-limited by a single-step Poisson process, where σ is the standard deviation.[39,40] The mean-normalized variance, r_{lo}, is 0.8 for the variable τ_{lo} (Table 1); thus, enzyme opening involves at least two elementary steps with similar, but not identical, rates.

Accordingly, we rule out the possibility of KF opening before the nucleotide incorporation step in KF's catalytic scheme. Instead, reopening of the fingers subdomain can be assigned to occur after nucleotide incorporation and at least one other step (Figure 1a). This assignment fits chemical expectations, and assumes that no significant steps are missing from the presented scheme. Future experiments will investigate τ_{lo} and r_{lo} under the influence of KF proofreading, which is unavailable to this exonuclease-disabled variant.

The mean duration $\langle \tau_{hi} \rangle$ of the enzyme's open conformation is 100-fold longer than $\langle \tau_{lo} \rangle$ and also sensitive to the identity of the Watson−Crick base pair (Figure 3b). $\langle \tau_{hi} \rangle$ is approximately 39 ms during the processing of either poly$(dG)_{42}$ or poly$(dC)_{42}$ templates, indicating that recognition of dCTP or dGTP by complementary, homopolymeric DNA templates are kinetically similar processes. Comparatively, the time required to form an A·T or T·A (A·T/T·A) base pair is almost twice as long as required for a G·C/C·G base pair. The value of $\langle \tau_{hi} \rangle$ grows to 64 and 71 ms for the recognition of dTTP or dATP respectively by complementary homopolymeric templates. Interestingly, these longer times for dATP/dTTP recognition have standard deviations of around 1.8%, much smaller than the approximately 15% observed for dCTP/dGTP recognition. In other words, the formation of a G·C/C·G base pair happens faster, but with much greater variability in the required duration.

The open conformation of KF, captured by τ_{hi}, includes several steps of the catalytic cycle (Figure 1a). For all four dNTPs, $r_{hi} = 1.0$. This value indicates that one rate-limiting step accounts for the majority of the $\langle \tau_{hi} \rangle$ value, though the open conformation lasts through many distinct steps of the catalytic cycle (Figure 1a). Previous work has established the rate-limiting step as the formation of an activated E*·DNA·dNTP

Table 1. Single-Molecule Kinetic Parameters for KF Processing Homopolymeric Templates[a]

template	nucleotide	τ_{lo} (ms)	r_{lo}	τ_{hi} (ms)	r_{hi}	H (nA)	rate (1/s)
poly$(dT)_{42}$	dATP	0.33 ± 0.08	0.85 ± 0.09	71.4 ± 1.4	0.95 ± 0.08	6.94	14.4 ± 2.9
poly$(dA)_{42}$	dTTP	0.42 ± 0.09	0.83 ± 0.06	63.7 ± 1.1	0.96 ± 0.06	4.90	16.0 ± 2.9
poly$(dG)_{42}$	dCTP	0.32 ± 0.07	0.78 ± 0.05	39.0 ± 5.6	0.98 ± 0.06	2.53	26.2 ± 4.4
poly$(dC)_{42}$	dGTP	0.33 ± 0.05	0.78 ± 0.05	38.0 ± 5.8	1.03 ± 0.07	2.40	28.5 ± 3.5

[a]Average values ± standard deviation.

complex during processive DNA synthesis.[33,34] Complementing these previous results, our measurements show that this rate-limiting step occurs during τ_{hi}. Thus, the activated E*·DNA·dNTP complex finishes forming prior to rapid closure of the fingers subdomain.

An average KF processing rate for each homopolymeric template is calculated in Table 1 from $\langle \tau_{lo} \rangle$ and $\langle \tau_{hi} \rangle$ values. The rates are approximately 2-fold faster for G·C/C·G than for A·T/T·A base pairs at 27 and 15 s^{-1}, respectively. The rates agree with ensemble measurements, particularly the observation of differences between dATP and dGTP incorporation.[21,22] The agreement suggests that tethering KF to a SWNT FET does not significantly alter the rate of enzymatic catalysis. Nevertheless, caution should be extended to interpretations of the values in Table 1. The extended single-molecule distributions of Figure 3 suggest a rate stability that may, in fact, be different for KF in its native environment or during processing of non-homopolymeric DNA templates.

The third independent parameter characterizing the closed conformation is the average height H of excursions in the transduced signal (Figure 3c). To depict the range of H values, histograms of $\Delta I(t)$ for each homopolymeric template were generated from 100-s recordings similar to those shown in Figure 2a,b. Each histogram is composed of a major peak associated with the higher-current, fingers-open conformation. A Gaussian fit to the poly(dC)$_{42}$ major peak is plotted below the four distributions to emphasize the wider $\Delta I(t)$ baseline distributions that accompany the longer $\langle \tau_{hi} \rangle$ values of processing poly(dA)$_{42}$ and poly(dT)$_{42}$ templates. This coupling suggests that the mechanism lengthening $\langle \tau_{hi} \rangle$ for A·T/T·A base pairs also involves conformational fluctuations that drive extra $\Delta I(t)$ fluctuations in the SWNT FET. Below the major peak, a minor, shoulder peak results from the excursions to the lower current, fingers-closed conformation. The position and width of this shoulder indicates the range of H values, the average of which is listed in Table 1 for each dNTP. All four shoulder distributions are different, with processing of poly-(dT)$_{42}$ being the most distinct in shape.

Based in part on our previous investigations of lysozyme-modified SWNT FETs,[41] we believe the average magnitude $\langle H \rangle$ is a proxy for the extent of mechanical closure by the enzyme. Specifically, movement of an enzyme's charged functionalities near the SWNT electrostatically gates the FET, and changes the magnitude of the corresponding $\Delta I(t)$ excursion. In the previous work with lysozyme, we demonstrated the sensitivity of the SWNT FET to small changes in the chemical environment within a 1.5 nm radius.[41] Assuming this rule remains true for KF, then differences in $\Delta I(t)$ result from different conformations accessed by the enzyme.

In this interpretation, tighter KF closures lead to larger H values during processing of poly(dT)$_{42}$ or poly(dA)$_{42}$ templates. Empirically, closure upon dGTP incorporation induces the smallest signal, less than half as large as closure upon dTTP and a small fraction of what can be observed with dATP during processing of their respective complementary homopolymeric templates. This observation could result from the enzyme's surface charges approaching closer to the SWNT during such incorporation events. Unfortunately, this ranking cannot be compared against X-ray structures for each ternary complex, which are not available for such transient states. However, structural data of KF bound to rNTPs and unnatural nucleotides show that the O-helix can adopt various distinct, closed conformations.[42] Taken together, the differences in

kinetic rates and $\Delta I(t)$ excursions distinguishing A·T/T·A from G·C/C·G base pairs demonstrate that KF fidelity relies on different conformations as a potential mechanism for verifying the correct Watson−Crick base pairs.

Finally, we conclude by noting that the three parameters discussed here have distinct mean values but substantially overlapping distributions. Neither τ_{lo}, τ_{hi}, nor H values are sufficient to identify incorporation of a particular dNTP with any degree of reliability. However, a combination of these parameters could provide better identification, and even opportunities for unique identification. Also, higher bandwidth resolution might reveal additional features in the $\Delta I(t)$ excursions, in order to distinguish one type of nucleotide from another. Thus, we believe that the SWNT FET technique for DNA sequencing with individual KF molecules deserves additional study, especially using dNTP mixtures and heteropolymeric DNA templates.

CONCLUSION

In conclusion, we report long duration, single-molecule measurements of KF replicating homopolymeric DNA templates during multiple rounds of turnover. Nucleotide-dependent kinetic rates and single-nucleotide resolution have been observed. The following observations provide new insights into the mechanism of KF-catalyzed bond formation: (1) The rate-limiting step for catalysis takes place during the open conformation prior to rapid closing of the fingers. (2) Only one rate-limiting step occurs during this open conformation. (3) Two conformations adjust the fit of the enzyme closing around either an A·T/T·A or a G·C/C·G base pair during phosphodiester bond formation. (4) Two or more steps occur during the KF closed conformation. Additional application of this technique should prove to be a powerful approach for uncovering the dynamics of KF and other enzymes, from processivity and kinetics to subtle and transient conformations.

ASSOCIATED CONTENT

⑤ Supporting Information

Materials and methods, bulk assays of enzymatic activity, and additional electronic signals and analysis. This material is available free of charge via the Internet at http://pubs.acs.org.

AUTHOR INFORMATION

Corresponding Author
gweiss@uci.edu; collinsp@uci.edu

Author Contributions
‡T.J.O. and Y.C. contributed equally.

Notes
The authors declare no competing financial interest.

ACKNOWLEDGMENTS

REFERENCES

(1) Steitz, T. A. *J. Biol. Chem.* **1999**, *274*, 17395−17398.
(2) Delagoutte, E. *Front. Biosci.* **2012**, *17*, 509−544.
(3) Tindall, K. R.; Kunkel, T. A. *Biochemistry* **1988**, *27*, 6008−6013.
(4) Bebenek, K.; Joyce, C. M.; Fitzgerald, M. P.; Kunkel, T. A. *J. Biol. Chem.* **1990**, *265*, 13878−13887.

(5) Mattila, P.; Korpela, J.; Tenkanen, T.; Pitkanen, K. *Nucleic Acids Res.* **1991**, *19*, 4967−4973.

(6) Joyce, C. M. *BBA-Protein Proteom.* **2010**, *1804*, 1032−1040.

(7) Aposhian, H. V.; Kornberg, A. *J. Biol. Chem.* **1962**, *237*, 519−525.

(8) Allen, D. J.; Benkovic, S. J. *Biochemistry* **1989**, *28*, 9586−9593.

(9) Christian, T. D.; Romano, L. J.; Rueda, D. *Proc. Natl. Acad. Sci. U.S.A.* **2009**, *106*, 21109−21114.

(10) Schwartz, J. J.; Quake, S. R. *Proc. Natl. Acad. Sci. U.S.A.* **2009**, *106*, 20294−20299.

(11) Torella, J. P.; Holden, S. J.; Santoso, Y.; Hohlbein, J.; Kapanidis, A. N. *Biophys. J.* **2011**, *100*, 1568−1577.

(12) Santoso, Y.; Joyce, C. M.; Potapova, O.; Le Reste, L.; Hohlbein, J.; Torella, J. P.; Grindley, N. D. F.; Kapanidis, A. N. *Proc. Natl. Acad. Sci. U.S.A.* **2010**, *107*, 715−720.

(13) Markiewicz, R. P.; Vrtis, K. B.; Rueda, D.; Romano, L. J. *Nucleic Acids Res.* **2012**, *40*, 7975−7984.

(14) Gill, J. P.; Wang, J.; Millar, D. P. *Biochem. Soc. Trans.* **2011**, *39*, 595−599.

(15) Berezhna, S. Y.; Gill, J. P.; Lamichhane, R.; Millar, D. P. *J. Am. Chem. Soc.* **2012**, *134*, 11261−11268.

(16) Kohlstaedt, L. A.; Wang, J.; Friedman, J. M.; Rice, P. A.; Steitz, T. A. *Science* **1992**, *256*, 1783−1790.

(17) Johnson, S. J.; Taylor, J. S.; Beese, L. S. *Proc. Natl. Acad. Sci. U.S.A.* **2003**, *100*, 3895−3900.

(18) Polesky, A. H.; Steitz, T. A.; Grindley, N. D. F.; Joyce, C. M. *J. Biol. Chem.* **1990**, *265*, 14579−14591.

(19) Purohit, V.; Grindley, N. D. F.; Joyce, C. M. *Biochemistry* **2003**, *42*, 10200−10211.

(20) McClure, W. R.; Chow, Y. In *Methods in Enzymology*, Vol. *64*; Daniel, L. P., Ed.; Academic Press: San Diego, 1980; pp 277−297.

(21) Detera, S. D.; Wilson, S. H. *J. Biol. Chem.* **1982**, *257*, 9770−9780.

(22) Bryant, F. R.; Johnson, K. A.; Benkovic, S. J. *Biochemistry* **1983**, *22*, 3537−3546.

(23) Kaushik, N.; Pandey, V. N.; Modak, M. J. *Biochemistry* **1996**, *35*, 7256−7266.

(24) Joyce, C. M.; Potapova, O.; DeLucia, A. M.; Huang, X.; Basu, V. P.; Grindley, N. D. F. *Biochemistry* **2008**, *47*, 6103−6116.

(25) Xie, S. N. *Single Mol.* **2001**, *2*, 229−236.

(26) Roy, R.; Hohng, S.; Ha, T. *Nat. Methods* **2008**, *5*, 507−516.

(27) Johnson, S.; Cain, S. *Appl. Opt.* **2008**, *47*, 5147−5154.

(28) Kong, X.; Nir, E.; Hamadani, K.; Weiss, S. *J. Am. Chem. Soc.* **2007**, *129*, 4643−4654.

(29) Choi, Y.; Moody, I. S.; Sims, P. C.; Hunt, S. R.; Corso, B. L.; Perez, I.; Weiss, G. A.; Collins, P. G. *Science* **2012**, *335*, 319−324.

(30) Choi, Y.; Moody, I. S.; Sims, P. C.; Hunt, S. R.; Corso, B. L.; Seitz, D. E.; Blaszczak, L. C.; Collins, P. G.; Weiss, G. A. *J. Am. Chem. Soc.* **2012**, *134*, 2032.

(31) Lu, H. P.; Xun, L. Y.; Xie, X. S. *Science* **1998**, *282*, 1877−1882.

(32) Lu, H. P. *Curr. Pharm. Biotechnol.* **2004**, *5*, 261−269.

(33) Wang, Y.; Lu, H. P. *J. Phys. Chem. B* **2010**, *114*, 6669−6674.

(34) Hu, D.; Lu, H. P. *Biophys. J.* **2004**, *87*, 656−661.

(35) Derbyshire, V.; Freemont, P.; Sanderson, M.; Beese, L.; Friedman, J.; Joyce, C.; Steitz, T. *Science* **1988**, *240*, 199−201.

(36) Kuchta, R. D.; Mizrahi, V.; Benkovic, P. A.; Johnson, K. A.; Benkovic, S. J. *Biochemistry* **1987**, *26*, 8410−8417.

(37) Dahlberg, M. E.; Benkovic, S. J. *Biochemistry* **1991**, *30*, 4835−4843.

(38) Joyce, C. M.; Benkovic, S. J. *Biochemistry* **2004**, *43*, 14317−14324.

(39) Svoboda, K.; Mitra, P. P.; Block, S. M. *Proc. Natl. Acad. Sci. U.S.A.* **1994**, *91*, 11782−11786.

(40) Xu, W. L.; Kong, J. S.; Chen, P. *J. Phys. Chem. C* **2009**, *113*, 2393−2404.

(41) Choi, Y.; Olsen, T. J.; Sims, P. C.; Moody, I. S.; Corso, B. L.; Dang, M. N.; Weiss, G. A.; Collins, P. G. *Nano Lett.* **2013**, *13*, 625−631.

(42) Wang, W.; Wu, E. Y.; Hellinga, H. W.; Beese, L. S. *J. Biol. Chem.* **2012**, *287*, 28215−28226.